

---

# Classification of Lung Nodules from Low Radiation CT scanned images

---

Hansori Chang, Shuming Cui, Yuhao Xue

Department of Biomedical Engineering

Duke University, Durham, NC, USA

hc270@duke.edu, sc653@duke.edu, yx161@duke.edu

## Abstract

In the project, we present a computer-aided detecting system that classifies lung nodules from CT scanned images with Poisson noise to simulate low radiation dose CT scan. The data used for the project is LIDC/IDRI dataset (screened by LUNA16 challenge). The CT scanned image is randomly cropped using selective search. Since there were too many images without a lung nodule, to balance the number, positive case images are manually cropped. They are resized into 64x64 to put into R-CNN with Alexnet. The network is first trained with the images from the dataset for the binary classification. For both normal images and Poisson noise images, high accuracies of classification are obtained. After that, the physical layer is added to apply Poisson noises to the images to test the model with low-quality images. For the localization, faster R-CNN with ResNet 50 is used for the model.

## 1. Introduction

According to the CDC, lung cancer is the second most common cancer for both men and women in the United States and it is the leading cause of cancer death: 24% of all cancer deaths<sup>[1]</sup>. To compare the survival rate of patients with the same stage of the same cancer type, the 5-year relative survival rate is being used. For lung cancer, the overall 5-year relative survival rate of all the Surveillance, Epidemiology, and End Result (SEER) stages combined is 24%<sup>[2]</sup>. At the distant stage, it is only 6%, but, if lung cancer is detected at the localized stage, the rate increases to 61% which is ten times higher<sup>[2]</sup>. Therefore, early detection of lung cancer is key for a patient's survival. At present, a computed tomography(CT) is widely used to detect the presence of a lung nodule in a patient's respiratory system<sup>[3]</sup>. Traditionally, ct scanned images are read by a diagnostic radiologist. The sensitivity of the diagnosis is highly dependent on the radiologist's skills and experience. Thus, computer-aided detection (CAD) with a machine learning algorithm is necessary<sup>[4]</sup>. The overall lung nodule detection has 4 stages: preprocessing of images, lung segmentation, lung nodule detection, and reduction of false positives<sup>[5]</sup>.

Moreover, CT uses X-rays that are ionizing radiation for imaging. A typical effective radiation dose of chest CT scan delivers 7mSv<sup>[6]</sup>. Since an average US citizen is exposed to 6.2 mSv annually and one chest x-ray delivers 0.007mSv, it is not a negligible amount of radiation dose<sup>[7-8]</sup>. It is demanding to enable lung nodule detection even with the low-dose ct scanned images. If an amount of radiation is decreased, the quality of the image will be lower. Thus, it is critical for the CAD system to perform well with low-quality images.

The goal of the project is to enable the classification of lung nodules in CT-scanned images. To simulate the low-dose radiation environment on the ct scan, images are blurred with Poisson noise, and the model will be trained and tested to classify lung nodules.

## 2. Data

The data used in this paper is Lung Nodule Analysis 2016 with the Lung Image Database Consortium image collection (LIDC-IDRI)<sup>[9]</sup>. It consists of lung cancer screening CT scans with annotated lesions. Among the CT scans, lung nodules with a thickness over 2.5mm are excluded; 888 CT scan mhd files will be used<sup>[9]</sup>. On the database, annotations are included from 4 radiologists, categorizing lesions as non-nodule, nodule<3mm, and nodule>3mm<sup>[9]</sup>. These annotations are used to refer to the standard of nodule detection.

## 3. Related Work

There are several relative research projects that have done lung nodule detection using machine learning algorithms. The overall structure of the project is significantly consistent among different projects. The major differences between the projects are the usage of different models of convolutional neural networks.

Li et al. have three major parts on the lung nodule detection method: Faster R-CNN. feature extraction models, and detection using faster R-CNN<sup>[10]</sup>. The Region Proposal Network (RPN) was used to deal with different aspects and scales of objects. In the paper, three feature extraction models are tested which are VGG16, ResNet50, and ResNet100.

Kopelowitz et al. adapted MaskRCNN for detection and segmentation of lung nodules<sup>[11]</sup>. Mask R-CNN, like a faster R-CNN, is two stages object detector: RPN and Region-based Convolutional Neural Network (RCNN). The backbone and RPN are trained together and only the second stage was trained later to make convergence faster. With the false-positive reduction, the model achieved a sensitivity of 0.936.

Girshick et al. introduced R-CNN. It combined region proposals with CNNs<sup>[12]</sup>. It gave 30% improvement on the best result on PASCAL VOC 2012 on object detection. It uses Alexnet for the feature extraction. Alexnet with R-CNN works well for the object detection and classification. Therefore, we decided to use R-CNN with Alexnet for our model.

## 4. Methods

### 4.1 Preprocess

The original images should be preprocessed before object detection. In order to train by R-CNN, the images should be resized first. The original size of our lung nodule dataset was 512 x 512. After a selective search, they are cropped into small pieces. However, the selective search created too many negative case images, probably because ct scanned images are only in greyscale. To balance the number of positive cases, we manually created positive cases by enlarging the lung nodule part of the image and then crop it into different images. We then resized the cropped pieces into 64 x 64 for further training.

### 4.2 R-CNN with AlexNet

We initially used the R-CNN model for object detection. The R-CNN model we used contains AlexNet which was designed by Alex Krizhevsky and it has a total of 8 layers: 5 convolution layers and 3 fully-connected layers<sup>[13]</sup>. Besides layers, there are 5 techniques that are used on the CNN model which are ReLU, dropout, overlapping pooling, local response normalization, and data augmentation. Relu nonlinearity function is used for all of the convolution and fully-connected layers. For an ideal AlexNet, local response normalization should be performed for modeling lateral inhibition in the actual cell environment, but, since TensorFlow doesn't use local response normalization due to training problems, we used batch normalization. Images are randomly cropped and reshaped into 64x64, instead of 224x224 to reduce memory usage in our environment. Since the input size is changed, we also had to adjust kernel

size from 11 to 10 and stride from 4 to 1 on the first convolution to obtain the same size of the image after the first convolution layer. To prevent overfitting, instead of average pooling, we used overlapping pooling and dropouts on the fully-connected layers. At the last, another sigmoid dense layer with 1 channel is added for binary classification. The preprocessed lung nodule images were trained for ROI pooling and then classified into two classifications: ‘Nodules’ or ‘No nodules’.

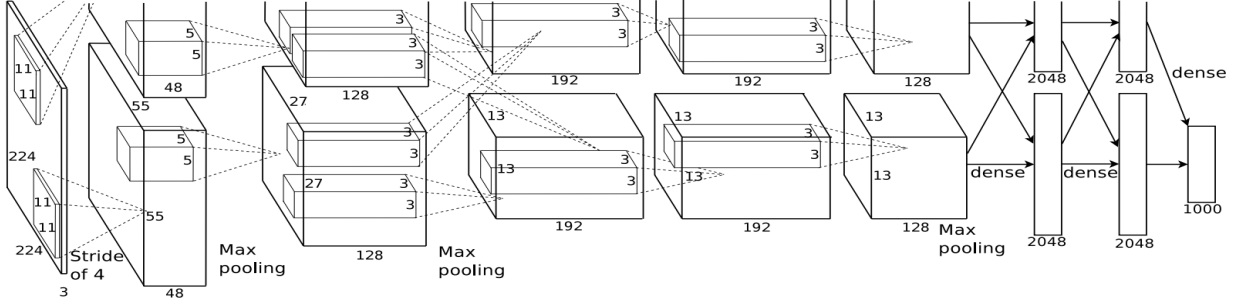


Figure 1. The structure of Alexnet<sup>[13]</sup>

### 4.3 Poisson noise

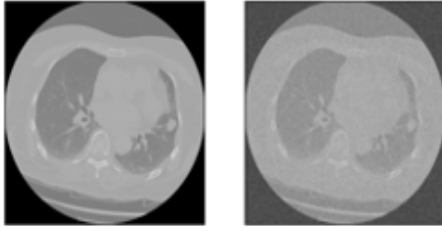


Fig 2. Original image and image with Poisson noise

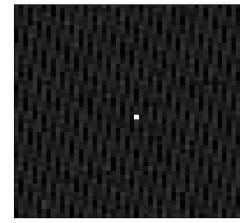


Fig 3. The Poisson convolution filter

As we mentioned in the proposal, we simply added the Poisson noise for the physical layer to simulate the low-dosage effect in CT-scan. In the current research on low-dose CT noise and denoising, the noise of CT images tends to be close to Poisson distribution, and denoising based on Poisson noise is often effective<sup>[14-15]</sup>. So we made a layer containing random Poisson noise to simulate the physical layer result from a low-dose CT scanner. Compared to a normal image blurring, the random noise we add is close to Poisson distribution. When the X-ray is weakened by low-dose, some X-ray that should have penetrated the tissue may disappear that causes a white noise, as well as enhancing the light noise that can make the result inaccurate. To add a random Poisson noise, we first imported the Skimage in python and then used the random noise function for one image. After that, we calculated the convolutional filter to apply consistent images to all the cropped images of one CT image.

### 4.4 Faster R-CNN

Based on the classification model, we wanted to observe if it is also effective for further investigation, localization of lung nodules on CT scan. Before moving forward, we planned to verify our approaches by modifying open source code from GitHub and then write our own algorithms<sup>[16]</sup>. First, we implemented R-CNN with Alexnet as our classification model, but we found out it fails to localize lung nodules. The result of the selective search contains too many negative samples, which were unable for AlexNet to complete feature selection. So we turned to another model called faster R-CNN that can be useful for nodule detection. For faster R-CNN, it requires the shorter side of images to be resized into 600 and keeps the length-width ratio. Our lung nodule images were resized into 600 x 600 for faster R-CNN training. The faster R-CNN network is much more complex than the R-CNN network. After the image is resized with a fixed length-width ratio, the backbone will be used to generate the feature map. The feature map (38 x 38 x 1024) will first be convoluted by a 3 x 3 layer with two 1 x 1 convolution layers followed.

One of the  $1 \times 1$  layers is used to determine if the selective frame contains objects and the other is used to adjust the frame. The generated proposal frame will be used with the feature map for the ROI pooling layer. The ROI pooling can generate feature layers for bbox regression and classification. There are several models that can be used for a faster R-CNN backbone, including VGG, ResNet, etc. We use the ResNet for lung nodule detection.

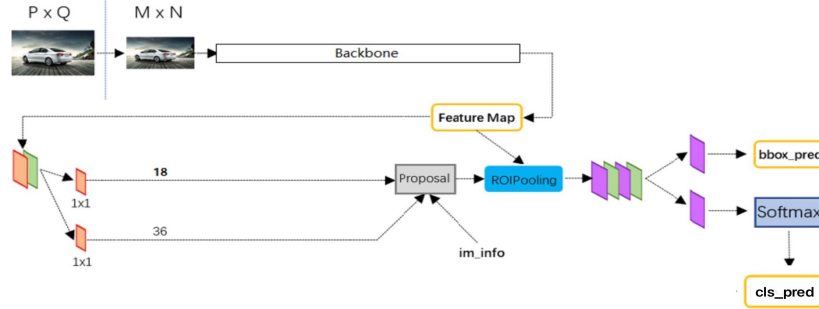


Fig 4. Structure of faster R-CNN model<sup>[16]</sup>

#### 4.5 Feature Extraction using ResNet50

The ResNet 50 includes two types of blocks: conv blocks and identity blocks. With the conv blocks being used to change the size of networks and identity blocks being used in series to improve the deep learning results.

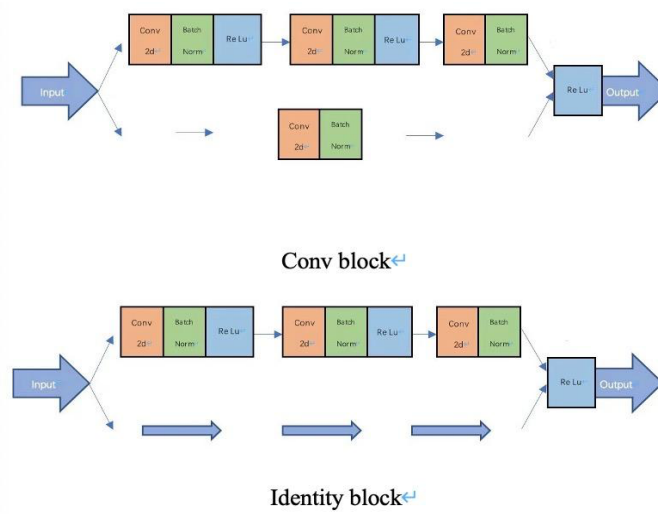


Fig 5. Structure of conv block and identity block

For our model, the input image will be resized to  $300 \times 300$  first by a 2-step convolution layer. After normalization and a ReLU function, it will be followed by a 2-step MaxPool stride before the convolution blocks and identity blocks. The ResNet will resize the image into  $38 \times 38$  with 1024 channels for bbox regression and classification. The ResNet we used for nodules detection contains 4 conv blocks and 9 identity blocks. Both conv blocks and identity blocks are implemented by using a bottleneck network, which contains three convolutions with corresponding batch normalization and a ReLU activation. The first convolution is  $1 \times 1$  with stride equals 1 to compress the channel of the image, the second convolution is  $3 \times 3$  with stride equals 1 and padding equals 1 to get the feature information of the image, and the last convolution is  $1 \times 1$  with no stride and the channel expands to 4 times of the input image channels. For the conv block, the convolution part in the residual path is implemented by a  $1 \times 1$

convolution with stride equals 1 and batch normalization. Because of the convolution part in the residual path, the conv block will change the size of the image, but not the identity layer.

The feature map is generated by the first three layers of the ResNet50, then after the proposal region is generated, the fourth layer will combine with the ROI pooling layer to do the classification and bbox regression.

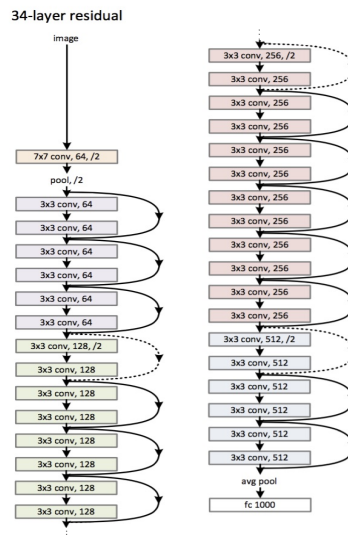


Fig 6. A sample structure of ResNet50

## 5. Results

### 5.1 Binary classification with R-CNN model and AlexNet

In the classification of CT scanned images, we used R-CNN with AlexNet. The loss and accuracy during training and validation are plotted below. The x-axis is the number of epochs. The final loss and accuracy are obtained. Sensitivity and precision are calculated from the confusion matrix.

#### 5.1.1 Non-noise dataset:

For the non-noise images, the final accuracies are 0.9805 for the training and 0.9358 for validation. The sensitivity is 0.9202 with the precision of 0.9445. This shows the model works well in classification with original images. However, the result of accuracy and loss showed trends of fluctuating. This is probably because the number of data we used was not big enough and the model may be overfitted.

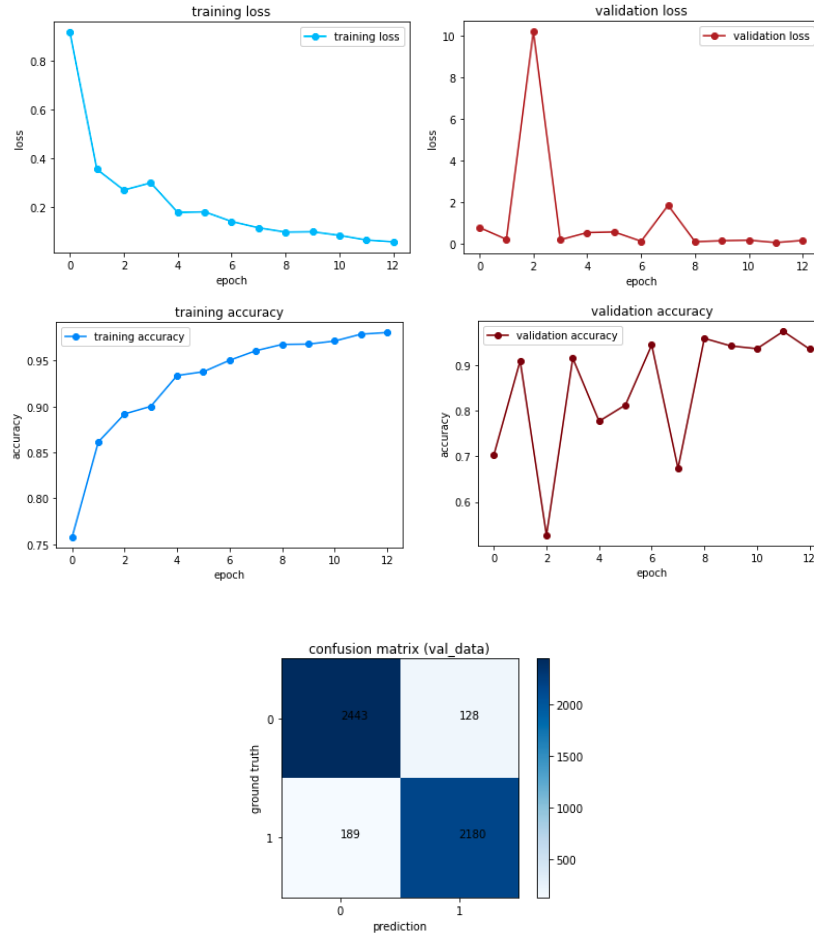


Fig 7. Classification result from images with noise

### 5.1.2 Noise dataset

The final accuracies are 0.9698 for the training and 0.8792 for validation. The sensitivity is 0.7907 with the precision of 0.9887. That shows our model can successfully classify the images. Although the sensitivity is not so high compared with precision, the model is still able to detect most non-nodule images.

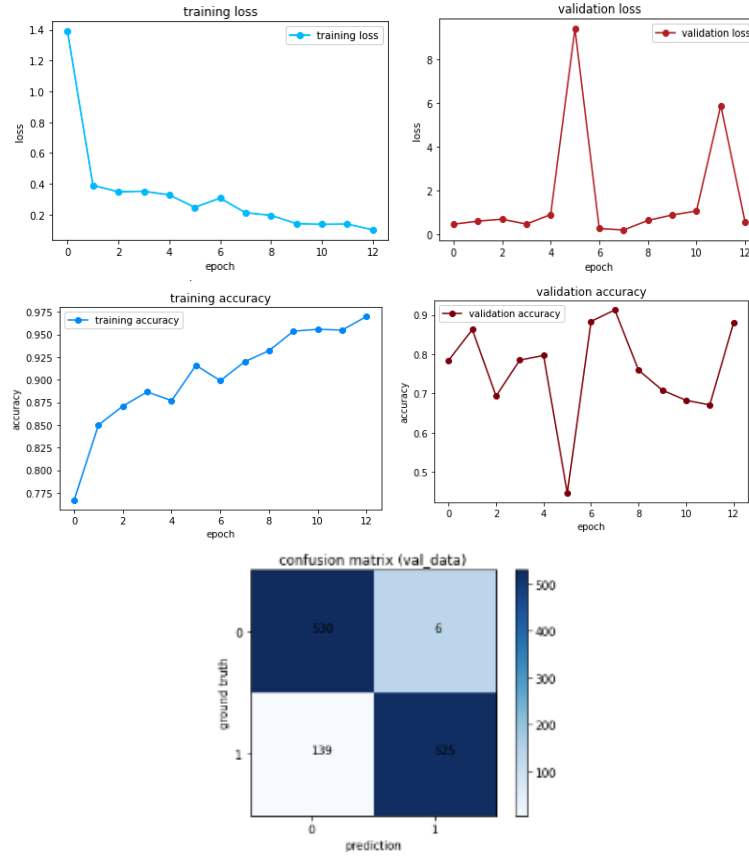


Figure 8. Classification result from images with noise

## 5.2 Object detection with faster R-CNN and ResNet50

We first conducted the selective search by R-CNN and AlexNet, but it failed to find the right location of the lung nodule.

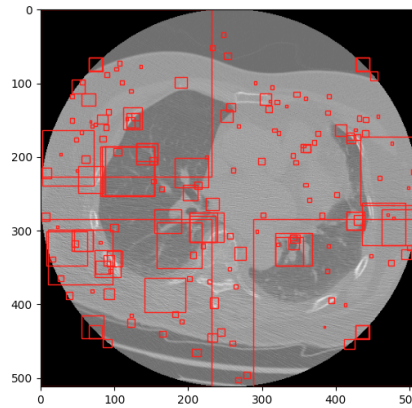


Fig 9. Result of selective search in R-CNN

Then we tried object detection with a faster R-CNN model. We detected the nodule from the lung image, but we only got a low mAP(mean average precision) for about 19%. The final precision is 0.3409 and the specification is 0.3913. Since the total loss was really low about 0.2 but the mAP was also really

low, after several attempts to solve this situation, we realized that we were unable to achieve the initial proposal. Also, we need more time and study on R-CNN for our proposal.

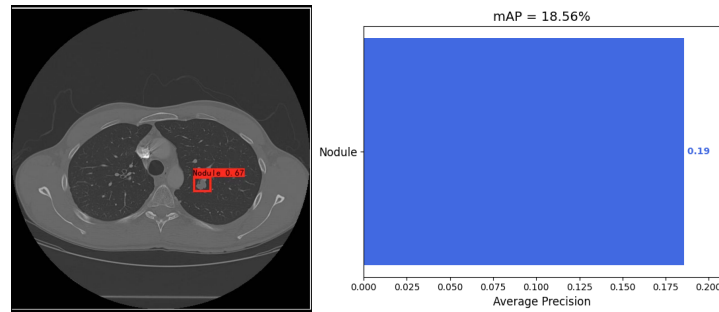


Fig 10. Result of object detection by faster R-CNN.  
Precision = 34.09%, specification = 39.13%

## 6. Discussion

To conclude, according to the accuracy and loss from the figure above, the model successfully classified lung nodules from CT scanned images both for normal images and images with Poisson noise. Both showed accuracy over 0.87, with high sensitivities. However, for object detection with faster R-CNN and ResNet50, it failed to find the lung nodule. Although it showed some results with localization, it required low mAP.

This study has potential limitations in that it didn't use all of the images on the dataset due to a large amount of time and memory needed. If it was trained with more datasets, we expect the outcome to be more stable and accurate. Also, false-positive reduction and support vector machines (SVM) are not performed on this model. Therefore, it still has room to improve its performance.

For further work, a model that performs the localization of the lung nodule's location can be written based on the knowledge from the literature. We have tried to model a localization, but it required a higher level of understanding and skills on machine learning algorithms than we expected. Also, in future development, we could add the physical layer to this model. With the physical layer optimized, the localization result could be more accurate because the model could try to optimize the difference between the nodule part and other parts of the image, such as decrease the similarity of color and texture. Our result has already shown that the classification shouldn't be a problem in low-dosage lung nodule detection, so the improvement of the proposal region will enhance the lung nodule, detection model. For the data augmentation process, rotation, and change of projection of images can be performed. Moreover, various feature extractions models such as VGG and ResNet can be used to compare different networks. For the last, as was mentioned above, the SVM and false positive reduction can be added to the current model to increase accuracy and sensitivity on lung nodule detection.



## 7. Reference

- [1] Torre L.A., Siegel R.L., Jemal A. (2016) Lung Cancer Statistics. In: Ahmad A., Gadgeel S. (eds) Lung Cancer and Personalized Medicine. Advances in Experimental Medicine and Biology, vol 893. Springer, Cham. [https://doi.org/10.1007/978-3-319-24223-1\\_1](https://doi.org/10.1007/978-3-319-24223-1_1)
- [2] *Cancer Facts & Figures*, Amer. Cancer Soc., Atlanta, GA, USA, 2012.
- [3] Rubin G. D. (2015). Lung nodule and cancer detection in computed tomography screening. *Journal of thoracic imaging*, 30(2), 130–138. <https://doi.org/10.1097/RTI.0000000000000140>
- [4] T. Messay, R. C. Hardie, and S. K. Rogers, "A new computationally efficient CAD system for pulmonary nodule detection in CT imagery," *Med. Image Anal.*, vol. 14, no. 3, pp. 390-406, 2010.
- [5] A. Chaudhary and S. S. Singh, "Lung Cancer Detection on CT Images by Using Image Processing," *2012 International Conference on Computing Sciences*, Phagwara, 2012, pp. 142-146, doi: 10.1109/ICCS.2012.43.
- [6] Vilar-Palop, J., Vilar, J., Hernández-Aguado, I., et al. (2016). Updated effective doses in radiology. *Journal of radiological protection : official journal of the Society for Radiological Protection*, 36(4), 975–990. <https://doi.org/10.1088/0952-4746/36/4/975>
- [7] Williams, P. M., & Fletcher, S. (2010). Health effects of prenatal radiation exposure. *American family physician*, 82(5), 488–493.
- [8] Deschênes, S., Charron, G., Beaudoin, G., et al. Diagnostic Imaging of Spinal Deformities: Reducing Patients Radiation Dose With a New Slot-Scanning X-ray Imager, *Spine*: April 20, 2010 - Volume 35 - Issue 9 - p 989-994 doi: 10.1097/BRS.0b013e3181bdcaa4
- [9] <https://luna16.grand-challenge.org/Data/>
- [10] Y. Li, L. Zhang, H. Chen and N. Yang, "Lung Nodule Detection With Deep Learning in 3D Thoracic MR Images," in *IEEE Access*, vol. 7, pp. 37822-37832, 2019, doi: 10.1109/ACCESS.2019.2905574.
- [11] Kopelowitz E, Engelhard G (2019) Lung nodules detection and segmentation using 3D Mask R-CNN. [arXiv:1907.07676](https://arxiv.org/abs/1907.07676)
- [12] Girshick, R., Donahue, J., Darrell, T., & Malik, J. (2014). Rich feature hierarchies for accurate object detection and semantic segmentation. In *Proceedings of the IEEE conference on computer vision and pattern recognition* (pp. 580-587).
- [13] A. Krizhevsky, I. Sutskever, and G. Hinton. Imagenet classification with deep convolutional neural networks. In NIPS, 2012.
- [14] Zhang Yuanke, Zhang Junying, Lu Hongbing,. Noise analysis and noise reduction for low-dose CT sinogram[J]. *Journal of Optoelectronics·Laser* ,2010, (7)
- [15] Zhao Mengliu, Li hongwei,. Image denoising based on Poisson-like noise model[J]. *Chinese Journal of Stereology and Image Analysis*, 2012, (1).
- [16] <https://github.com/bubliiiiing/faster-rcnn-pytorch>